

Probing the ρ^0 Mass Modification in the Subthreshold Region on ${}^3\text{He}$

G. M. Huber, G. J. Lolos, and Z. Papandreou

Department of Physics, University of Regina, Regina, Saskatchewan, S4S 0A2 Canada

(Received 8 December 1997)

An earlier measurement of the ρ^0 mass in the nuclear medium, reported by the TAGX Collaboration, indicated a substantial mass reduction of $\delta m_{\rho^0} = 160 \text{ MeV}/c^2$ in the ${}^3\text{He}(\gamma, \pi^+\pi^-)$ reaction. In this Letter, we report the reanalysis of previously published data for the same reaction at lower photon energies, $E_\gamma = 380\text{--}700 \text{ MeV}$, which lie below the $\rho^0 \rightarrow \pi^+\pi^-$ detection threshold unless the ρ^0 mass is significantly modified by the nuclear medium. We find the resulting mass shift in this region to be even larger, $\delta m_{\rho^0} = 280 \pm 40 \text{ MeV}/c^2$, consistent with ρ^0 decay in the field of the nucleon as the dominant effect. [S0031-9007(98)06384-4]

PACS numbers: 24.85.+p, 12.40.Yx, 25.20.Lj

It has been established by chiral perturbation theory (χ PT) that, at infinite nuclear matter density, deconfinement of the quarks takes place and hadron masses are reduced to zero. Correspondingly, at some high nuclear matter density ρ_c , partial restoration of chiral symmetry takes place [1]. One of the consequences of this restoration is a reduction of the vector meson masses within the nuclear medium, a topic that has been the focus of intense interest within the theoretical community, as outlined in a recent review [2]. There is qualitative agreement among most theoretical predictions that the renormalized vector meson mass is reduced in the nuclear medium.

Several heavy ion collider experiments at CERN (CERES, HELIOS, and NA28), leading to dilepton production, indicate an enhanced production cross section in the lower dilepton invariant mass range of $200\text{--}600 \text{ MeV}/c^2$ [3]. The spectral shapes are not well reproduced by theoretical calculations based on hadron decay after freeze out when employing free particle properties. The dominant $\pi^+\pi^-$ annihilation mechanism fails to account for the observed excess dilepton production, and better agreement is found if the ρ^0 mass is modified [4], according to the scaling hypothesis of Brown and Rho [5], or according to quark sum rules (QSR) predictions [6]. Alternate explanations have been proposed [7] which also depend on a decrease of the ρ^0 meson mass. However, theoretical issues still remain open in such complex reactions [3].

An IUCF experiment has reported evidence of a substantially reduced $m_{\rho^0}^*$, using polarized proton scattering on ${}^{28}\text{Si}$ [8]. An improvement between the data and calculations was observed if the ρ^0 mass is reduced by 20% in nuclear matter. This improvement, however, did not carry through to all of the observables. Questions can be raised regarding the interpretation of this result, such as the definition of mass when the ρ^0 is in the propagator, as well as the issue of ρ^0 - ω interference, and the effect of the medium on the ω mass. Recent Bonn results also indicate a significant reduction in the total photoabsorption cross section per nucleon on various nuclei [9], which

could be explained by a corresponding decrease of the ρ^0 mass in nuclear medium. All such evidence of a ρ^0 mass renormalization is, however, indirect and inconclusive.

A more conclusive and direct measurement is needed, involving the formation of the invariant mass of the ρ^0 in a simpler nuclear system, where the interpretation of the results is less complex and less model dependent. Photoproduction of the ρ^0 on ${}^3\text{He}$ fulfills this role. The ρ^0 meson is characterized by a short lifetime, and a decay into two charged particles, which simplifies the detection techniques. With a decay length of $c\tau = 1.3 \text{ fm}$, a large portion of the produced ρ^0 mesons will decay within the nuclear environment at low Lorentz boost.

Photoproduction of the ρ^0 on a proton has a threshold of approximately 1080 MeV , assuming a well-defined free mass of $768 \text{ MeV}/c^2$. At tagged photon energies below 1080 MeV , the coherent process ${}^3\text{He}(\gamma, \pi^+\pi^-){}^3\text{He}$ is suppressed, and the probability of production on an individual nucleon inside the nucleus is enhanced, thus ensuring that the ρ^0 has been produced within the nuclear medium. In addition, by taking advantage of the bound nucleon's Fermi momentum to produce the ρ^0 , the latter is produced with small Lorentz boost with respect to the nuclear medium, thus increasing the probability of decay within the medium. We refer to this process as "subthreshold production," as it can occur below the free production threshold.

Results from a ρ^0 photoproduction experiment on ${}^3\text{He}$ in the $E_\gamma = 800\text{--}1120 \text{ MeV}$ energy region have recently been published by the TAGX collaboration [10]. The results are consistent with a significant mass reduction of $\delta m_{\rho^0} = 160 \pm 35 \text{ MeV}/c^2$. The same collaboration has also published double pion photoproduction cross section results from ${}^3\text{He}$ at lower photon energies, $E_\gamma = 380\text{--}700 \text{ MeV}$ [11]. Both works make use of a tagged photon beam, and a large solid angle magnetic spectrometer which is optimized for coplanar reactions [12]. Assuming free values for the mass and width of the ρ^0 , no events from the decay of this meson should contribute to the $E_\gamma = 380\text{--}700 \text{ MeV}$ data, as they lie below the

threshold of the ${}^3\text{He}(\gamma, \rho^0)$ reaction. For this reason, the analysis of Ref. [11] did not incorporate the ρ^0 channel. However, with the results from Ref. [10] consistent with a substantially reduced $m_{\rho^0}^*$, it is conceivable that the ρ^0 channel will contribute to this data sample if the ρ^0 mass is substantially shifted downwards. Here, we present the results of a reanalysis of the data in Ref. [11] to see if it supports or rejects this hypothesis.

The reanalysis of the low energy data is similar in philosophy to the higher energy analysis of Ref. [10]. We have taken the reaction channels included in the original analysis of Ref. [11] and added to them channels incorporating a ρ^0 with a medium modified mass. The original processes are as follows [where sp denotes the spectator nucleon(s)]:

(1) Δ_{1232} production via $\gamma + {}^3\text{He} \rightarrow \Delta\pi(NN)_{sp} \rightarrow \pi^+\pi^-ppn$.

(2) Quasifree N_{1440}^* (Roper) production, which decays via the reaction $N^* \rightarrow \pi^+N$, following its production in the $\gamma + {}^3\text{He} \rightarrow N_{1440}^*\pi^-(NN)_{sp}$ reaction.

(3) Double Δ_{1232} production via the reactions $\gamma + {}^3\text{He} \rightarrow \Delta\Delta p_{sp}$, followed by $\Delta\Delta p_{sp} \rightarrow \pi^+\pi^-ppn$.

(4) Double pion production associated with ppn (${}^3\text{He}$) final states. This process proceeds via the reaction $\gamma + {}^3\text{He} \rightarrow \pi^+\pi^-ppn$ ($\pi^+\pi^-{}^3\text{He}$), following five (three) body phase space, and is referred to as 5BPS (3BPS).

Monte Carlo (MC) simulations were performed for all of the above mentioned reactions. As MC simulations assume constant matrix elements for each modeled process, the shape of each distribution is defined by the appropriate (kinematical) phase space. In order to ensure constancy of the matrix elements, the photon energy bins should be as narrow as possible, consistent with meaningful statistics of the data in these energy bins. In the earlier analysis [11], it was determined that 80 MeV wide energy bins satisfy both requirements, and this was retained. Thus, the tagged photon energy range of 380–700 MeV available to the experiment is divided into four incident energy bins of 380–460, 460–540, 540–620, and 620–700 MeV. Each energy bin is treated independently from the others.

Generally speaking, the upper energy bins are dominated by resonant production mechanisms, while non-resonant mechanisms dominate very close to the $\pi^+\pi^-$ production threshold. Reference [11] found that the lowest photon energy bin data are strongly supportive of the coherent $\gamma + {}^3\text{He} \rightarrow \pi^+\pi^-{}^3\text{He}$ reaction (3BPS). The breakup channel, $\gamma + {}^3\text{He} \rightarrow \pi^+\pi^-ppn$ (5BPS), was also used in the analysis. 5BPS-like two-pion production can, in principle, be accounted for by a superposition of all available N^* and Δ channels, but near threshold, it is not possible to experimentally distinguish the distinct nucleonic excitation processes. Thus, we have retained 3BPS in the data analysis as a distinctly separate production process.

Five observables of interest were extracted from the MC simulations: invariant mass of the two-pion sys-

tem $m_{\pi\pi}$, missing mass m_{miss} , missing momentum p_{miss} , opening angle between the two pions $\theta_{\pi\pi}$, and emission angle of the two-pion momentum vector with respect to the beam θ_{IM} . The MC fitting procedure required the simultaneous fitting of all five observables to the data. Despite the sophistication of the simulations and the MC fitting procedure, the earlier analysis of Ref. [11] was unable to obtain a perfect fit to every observable. For example, even though the fit-extracted Δ and $\Delta\Delta$ total cross sections were consistent with expectations from experiments on proton and deuterium targets, small but persistent discrepancies remained between the shapes of the MC sum fits and the data observable distributions. The missing momentum variable was the least satisfactorily fit, with an experimental distribution that is narrower than the sum of the fit simulations.

Unlike in the original analysis of Ref. [11], where the MC simulations were fit only to the total $\pi^+\pi^-$ yield distributions, in the present work m_{miss} and $\theta_{\pi\pi}$ cuts were introduced (MC determined), as in Ref. [10]. As $\rho^0 \rightarrow \pi^+\pi^-$ occurs back-to-back in the ρ^0 rest frame, a cut selecting large $\pi^+\pi^-$ opening angle events will enhance the contribution of any ρ^0 channels compared to the other $\pi^+\pi^-$ production processes. m_{miss} cuts also improved the sensitivity of the analysis by restricting the contribution of energetic nucleon emission from Δ and N^* decay. In all cases, the MC simulated data were analyzed in exactly the same way as the experimental data.

The five quantities $m_{\pi\pi}$, m_{miss} , $\theta_{\pi\pi}$, θ_{IM} , and p_{miss} were fit simultaneously for both the unselected (total) two-pion data and the selected (ρ^0 enhanced) data for each incident photon energy bin. As a result of this fitting process, the simulations are very constrained, since different processes populate different regions of phase space for the five extracted observables. The ρ^0 mass was iterated over values from 400 to 768 MeV/ c^2 and the goodness of fit (χ^2) calculated for each.

In summary, all of the channels used in the Watts *et al.* [11] analysis were retained for consistency with the earlier analysis, and to reflect the dominant physics processes at these incident photon energies. Processes with ρ^0 ${}^3\text{He}$ and $\rho^0 p(pn)_{sp}$ final states with reduced $m_{\rho^0}^*$ were added to the analysis, and the contributions of all of the channels reoptimized to produce the best fit to the data, remaining consistent with the previously published cross sections. However, the data only showed evidence for the $\rho^0 p(pn)_{sp}$ channel; there was no evidence for events from the ρ^0 ${}^3\text{He}$ channel. This is in agreement with the findings of Lolos *et al.* [10] that the coherent (${}^3\text{He}$) region was consistent with a smaller mass shift than the ppn region, which would put its energy threshold above that available in this data set.

We employed two different methods of fitting the MC simulations to the data, which produced similar results. Figure 1(a) shows the goodness of fit for the average of the two fitting procedures versus $m_{\rho^0}^*$. The inclusion

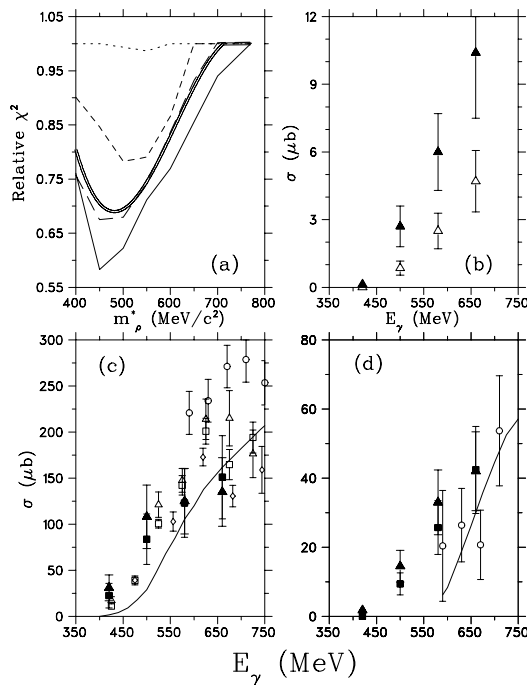


FIG. 1. Panel (a) shows the χ^2 of the fitting as a function of $m_{\rho^0}^*$ for the four energy bins. The dotted, short-dashed, long-dashed, and solid curves represent the 380–460, 460–540, 540–620, and 620–700 MeV bins, respectively. The double curve is a fit to the average for 460–700 MeV. Panel (b) shows cross sections for the $\rho^0 p p n$ contributions of this work assuming $m_{\rho^0}^* = 500$ (solid triangles) and $m_{\rho^0}^* = 600$ MeV/ c^2 (open triangles). Panel (c) shows cross sections for the sum of Δ and N^* , and panel (d) for $\Delta\Delta$ processes, assuming a modified ρ^0 mass of 500 MeV/ c^2 (solid triangles). The original analysis data [11] are indicated by the solid squares. Other previous related works referred there (proton and deuterium target data and calculations multiplied by the appropriate target weighting factor $3/A_{\text{tgt}}$) are also shown for comparison.

of the modified mass $\rho^0 \rightarrow \pi^+ \pi^-$ process significantly improved the χ^2 of the distributions over the original analysis of Ref. [11], which corresponds to the unaltered mass of the ρ^0 of 768 MeV/ c^2 . The best MC fit to the data distributions occurs at $m_{\rho^0}^* = 490 \pm 40$ MeV/ c^2 , which is even lower than the $m_{\rho^0}^* = 610$ MeV/ c^2 of Ref. [10].

Figure 1(a) also illustrates the interplay between E_γ and $m_{\rho^0}^*$ in terms of the ρ^0 production energy threshold. The $E_\gamma = 460$ –540 MeV data, for example, lie below the $\rho^0 \rightarrow \pi^+ \pi^-$ threshold for $m_{\rho^0}^* \geq 650$ MeV/ c^2 , and so the quality of fit is unaffected for ρ^0 masses in this region. For ρ^0 masses below 650 MeV/ c^2 , the $\rho^0 p(pn)_{sp}$ channel can contribute, and the quality of fit for this energy bin improves. The highest photon energy bin (620–700 MeV) is accessible to all ρ^0 masses below the free value, while the lowest photon energy bin (380–460 MeV) is largely insensitive to any ρ^0 mass shift. Thus, in the photon energy regime where the reaction threshold is a less significant effect ($E_\gamma > 540$ MeV), the $m_{\rho^0}^*$ values obtained are fairly consistent. In the

lower energy region, the effect of the reaction threshold is greater, and the extracted $m_{\rho^0}^*$ value less certain. The 40 MeV/ c^2 mass uncertainty was determined from the level of sensitivity of the fitting procedure to the various values of $m_{\rho^0}^*$ assumed to make this panel, for $E_\gamma > 460$ MeV.

In all cases, total cross sections were extracted from the fits to the data set and compared to those in the literature, as shown for the two dominant $\pi^+ \pi^-$ production channels in panels 1(c) and 1(d). The very good agreement between the results obtained by this analysis and those of the previous one in Ref. [11], as well as to the world data, verifies the reliability of the analysis and provides a constraint to the fitting procedure. The small differences between the σ_Δ and $\sigma_{\Delta\Delta}$ of this work and those of Ref. [11] also indicate the small sensitivity of these cross sections to $m_{\rho^0}^*$ and the relatively small overall contribution to $\sigma_{\pi\pi}$ from ρ^0 decay in this energy region. Figure 1(b) shows the cross section attributed to the $\rho^0 p p n$ process for two different possible values of $m_{\rho^0}^*$. As expected, the ρ^0 production cross section increases as $m_{\rho^0}^*$ is decreased [7], because of the larger available phase space for ρ^0 production.

Figure 2 compares the fits of the simulations to the total $E_\gamma = 620$ –700 MeV data set, assuming $m_{\rho^0}^* = 500$ MeV/ c^2 [panels 2(a) and 2(b)] and assuming the free

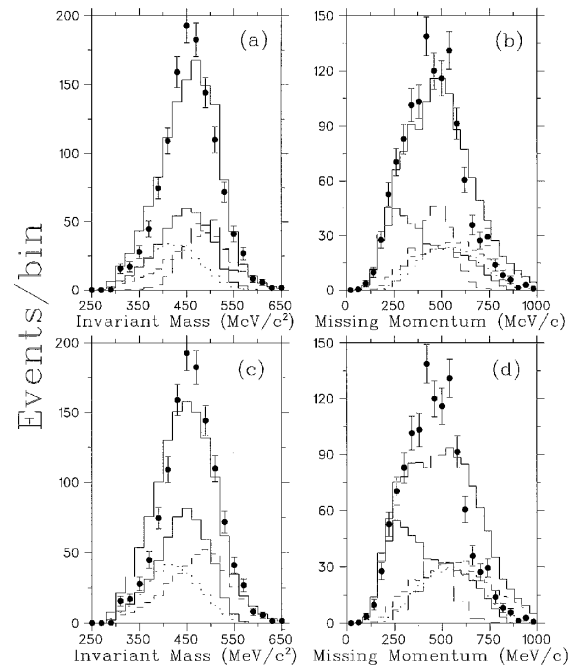


FIG. 2. Data and MC fit distributions for invariant mass and missing momentum from the photon energy bin of 620–700 MeV. Panels (a) and (b) assume $m_{\rho^0}^* = 500$ MeV/ c^2 , while panels (c) and (d) assume that the m_{ρ^0} takes only its free value. The solid circles correspond to the data, while the lower solid line is the sum of the Δ and N^* mechanisms, the short-dashed line is the $\Delta\Delta$ mechanism, the dotted line is the sum of 3BPS and 5BPS, and the long-dashed line is the $\rho^0 p p n$ mechanism. The upper solid line is the sum of the simulations.

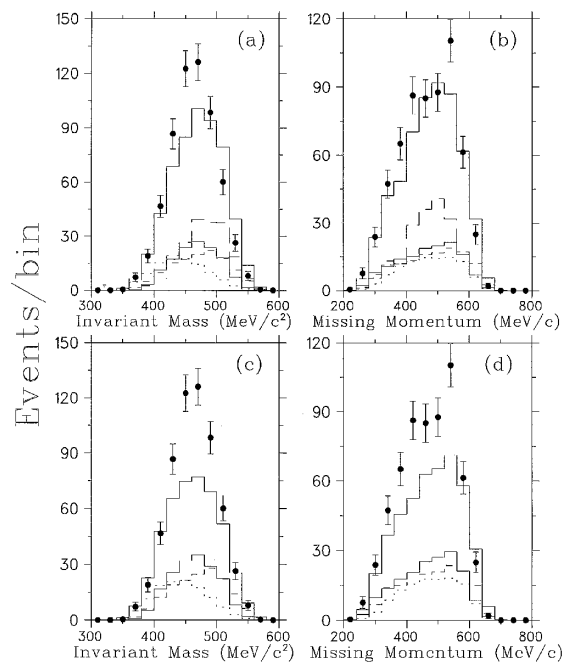


FIG. 3. Same as for Fig. 2, but for the ρ^0 enhanced data set by the application of $\theta_{\pi\pi} \geq 70^\circ$ and $2860 \leq m_{\pi\pi} < 2980$ MeV/ c^2 cuts as described in the text.

ρ^0 mass only [panels 2(c) and 2(d)]. Figure 3 shows the same MC simulations, with the normalizations determined by the fitting in Fig. 2, but now with the ρ^0 enhanced $\pi^+\pi^-$ cuts mentioned earlier. The contributions of the competing $\pi^+\pi^-$ production channels have been optimized in both cases, so what is presented is the best possible fit to the data given the reaction channels available. There are still some discrepancies between the sum of the MC fits and the data, but the improvement in the fit is significant, consistent with the improvement in the χ^2 shown in Fig. 1(a). The improvement in the fit to the missing momentum is especially pronounced.

It should be noted that it is the selectivity of the TAGX detector to coplanar reactions which allows a small σ_{ρ^0} to play such a large role in the fitting of the $\pi^+\pi^-$ data set relative to the much larger σ_{Δ} and $\sigma_{\Delta\Delta}$. Of the available production channels, only ρ^0 decay results in the intrinsically coplanar emission of a $\pi^+\pi^-$ pair, resulting in a much larger detection acceptance for this reaction than for the other competing channels, thus optimizing the sensitivity of the data sample for this $m_{\rho^0}^*$ study.

We have also investigated the role of ρ^0 - N relative dynamics in this low energy region of ρ^0 photoproduction. Quasifree ρ^0 production via the reaction $\gamma + N(NN)_{sp} \rightarrow \rho^0 N'(NN)_{sp}$ has been simulated with the same MC programs used for the data analysis. For $E_\gamma = 620$ – 700 MeV, the mean relative momentum p_{ρ^0-N} is 180 MeV/ c , which corresponds to a mean decay length of 0.3 fm for the ρ^0 . Thus, the ρ^0 decays within the

field of the interacting nucleon, and the effective hadronic matter density is that of the nucleon, rather than the mean nuclear field [13]. This explanation accounts qualitatively for the lower $m_{\rho^0}^*$ in this work, compared to our higher energy work in Ref. [10]. In either energy regime, the mass shift is much larger than predicted for ${}^3\text{He}$ using the nuclear mean field alone [14].

A recent paper [15] further supports our explanation of the low $m_{\rho^0}^*$ extracted in this work. The authors of this paper show that chiral restoration, corresponding to $m_\rho^* = 0$, should occur at an energy density $\epsilon \geq 1$ GeV/ fm^3 . Chiral and cloudy bag models of the nucleon indicate that the nucleonic density is approximately this value, and greater than that claimed to be necessary for chiral restoration. Although the ρ^0 may be massless in the interior, it is likely to be produced near the nucleon's surface. There the ρ meson mass will be low, qualitatively consistent with our result.

In conclusion, we have reanalyzed data from the ${}^3\text{He}(\gamma, \pi^+\pi^-)$ reaction published earlier [11] by including a ρ^0 with modified mass. The results are consistent with a large mass shift, indicating that the hadron density at the decay vertex is much higher than expected. A plausible explanation is offered by the decay of the ρ^0 within the strong nucleonic field at low relative ρ^0 - N momenta.

The authors acknowledge the very useful discussions with P. Guichon, M. Ericson, and A. Thomas during the Workshop on Hadrons in Dense Matter (Adelaide, March 10–28, 1997).

-
- [1] G. E. Brown *et al.*, Nucl. Phys. **A343**, 295 (1995).
 - [2] T. Hatsuda and T. Kunihiro, Phys. Rep. **247**, 221 (1994).
 - [3] A. Drees, Nucl. Phys. **A610**, 536 (1996).
 - [4] G. Q. Li, C. M. Ko, and G. E. Brown, Phys. Rev. Lett. **75**, 4007 (1995).
 - [5] G. E. Brown and M. Rho, Phys. Rev. Lett. **66**, 2720 (1991).
 - [6] W. Cassing, W. Ehehalt, and C. M. Ko, Phys. Lett. B **363**, 35 (1995).
 - [7] G. Chanfray, R. Rapp, and J. Wambach, Phys. Rev. Lett. **76**, 368 (1996).
 - [8] E. J. Stephenson *et al.*, Phys. Rev. Lett. **78**, 1636 (1997).
 - [9] M. Mirazita *et al.*, Phys. Lett. B **407**, 225 (1997).
 - [10] G. J. Lolos *et al.*, Phys. Rev. Lett. **80**, 241 (1998); Z. Papandreou *et al.* (to be published).
 - [11] D. G. Watts *et al.*, Phys. Rev. C **55**, 1832 (1997).
 - [12] K. Maruyama *et al.*, Nucl. Instrum. Methods Phys. Res., Sect. A **376**, 335 (1996).
 - [13] P. A. M. Guichon and M. Ericson (private communication).
 - [14] K. Saito, A. W. Thomas, and K. Tsushima, Phys. Rev. C **56**, 566 (1997).
 - [15] G. E. Brown, M. Buballa, and M. Rho, Nucl. Phys. **A609**, 519 (1996).